



X Workshop on Particle Correlation and Femtoscopy 25-29 August, 2014

Higher flow harmonics and ridge effect in PbPb collisions with HYDJET++ model

Gyulnara Eyyubova,

Czech Technical University in Prague & SINP MSU, Russia

V.L. Korotkikh, I.P. Lokhtin, S.V. Petrushanko, A.M. Snigirev
SINP MSU



esf european
social fund in the
czech republic



EUROPEAN UNION



MINISTRY OF EDUCATION,
YOUTH AND SPORTS

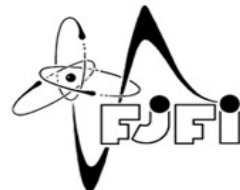


OP Education
for Competitiveness

INVESTMENTS IN EDUCATION DEVELOPMENT

Project OPVK

CZ.1.07/2.3.00/30.0034



Outline

- HYDJET++ model (hydro + jet)
- Description of elliptic flow v_2
- Triangular flow v_3 and higher flow harmonics
- Dihadron angular correlations
- Conclusions

HYDJET++ model

*I.Lokhtin, L.Malinina, S.Petrushanko, A.Snigirev, I.Arsene, K.Tywoniuk,
Comp. Phys. Comm. 180 (2009) 779*

The model combines hard and soft physics.

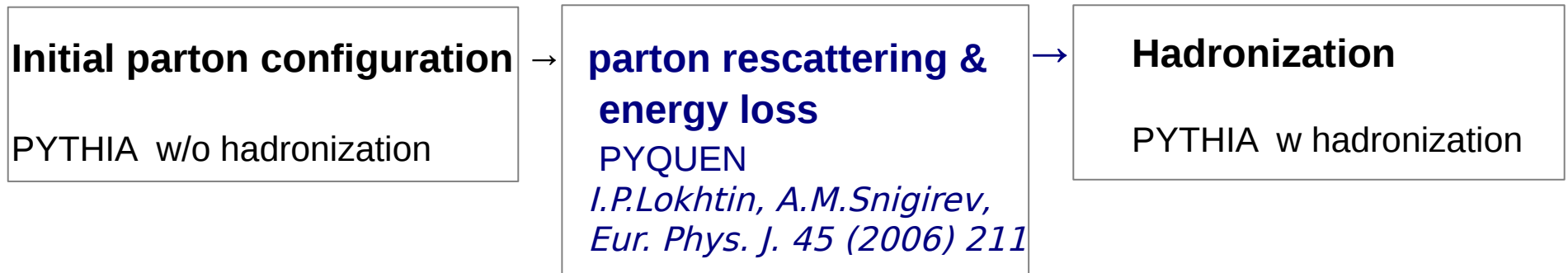
1. Soft part

Hadronization from freez-out surface with distribution function:

$$f_i^{\text{eq}}(p^{*0}; T^{\text{ch}}, \mu_i, \gamma_s) = \frac{g_i}{\gamma_s^{-n_i^s} \exp([p^{*0} - \mu_i]/T^{\text{ch}}) \pm 1}$$

p^{*0} is the hadron energy in the fluid element rest frame, γ_s is strangeness suppression factor

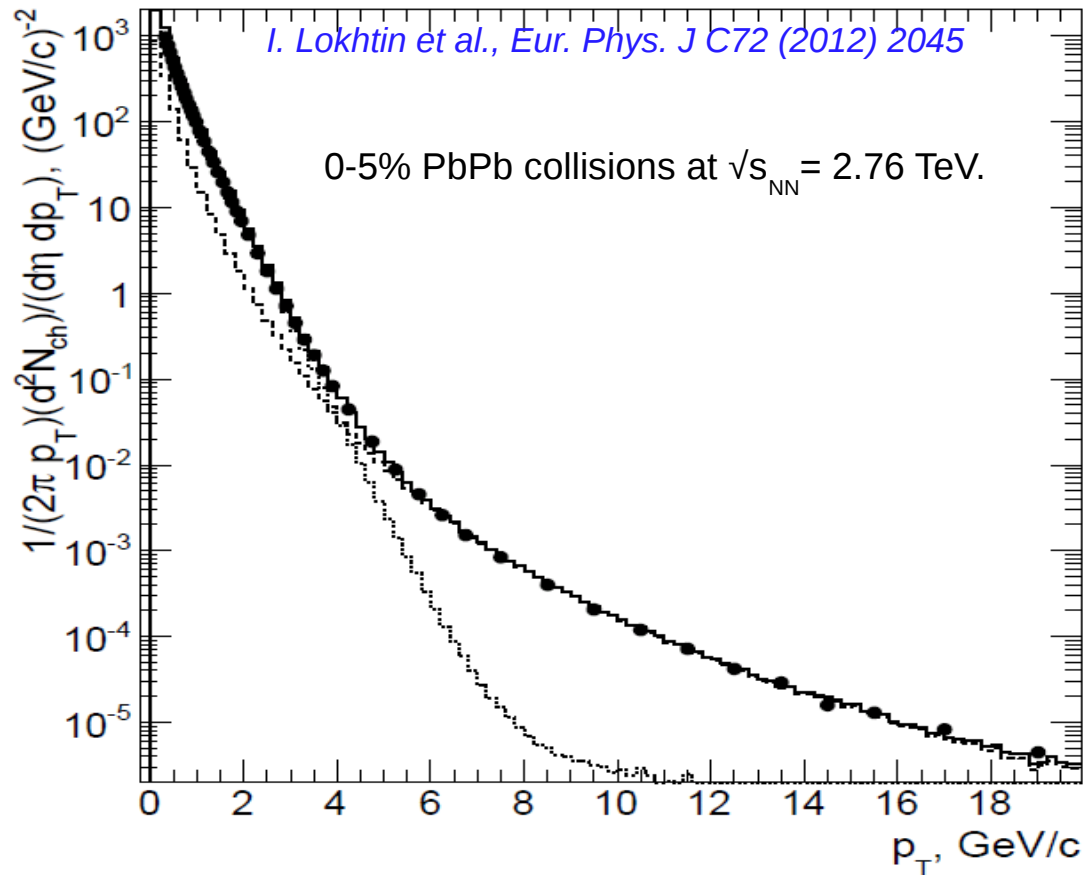
2. Hard part



- ◆ Parton collisional loss
- ◆ Radiative loss

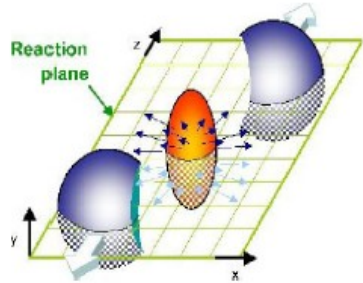
HYDJET++ model

The contribution of soft and hard components into total multiplicity depends on a model parameter: **minimal p_T of hard process.**



The points are ALICE data, histogram dashed is hard component, dotted is soft component of HYDJET++.

HYDJET++ model: elliptic flow



$$\frac{dN}{d\varphi} = \frac{1}{2\pi} \left(1 + \sum 2v_n(p_t) \cos(n[\varphi - \Psi_n]) \right)$$

Soft part:

- Space modulation of freeze-out surface;
- Modulation of liquid velocities on the surface

$$v_2 \propto \frac{2(\delta - \epsilon)}{(1 - \delta^2)(1 - \epsilon^2)}$$

Space asymmetry:

$$\epsilon(b) = \frac{R_y^2 - R_x^2}{R_y^2 + R_x^2}$$

$R(b)$ is radius of the freeze-out surface

Momentum asymmetry:

$$\tan \varphi_* = \sqrt{\frac{1 - \delta(b)}{1 + \delta(b)}} \tan \varphi$$

φ_u : azimuthal angle of liquid velocity vector

φ : space azimuthal angle

Parameters $\epsilon(b_0)$, $\delta(b_0)$ are tuned to describe experimental data.

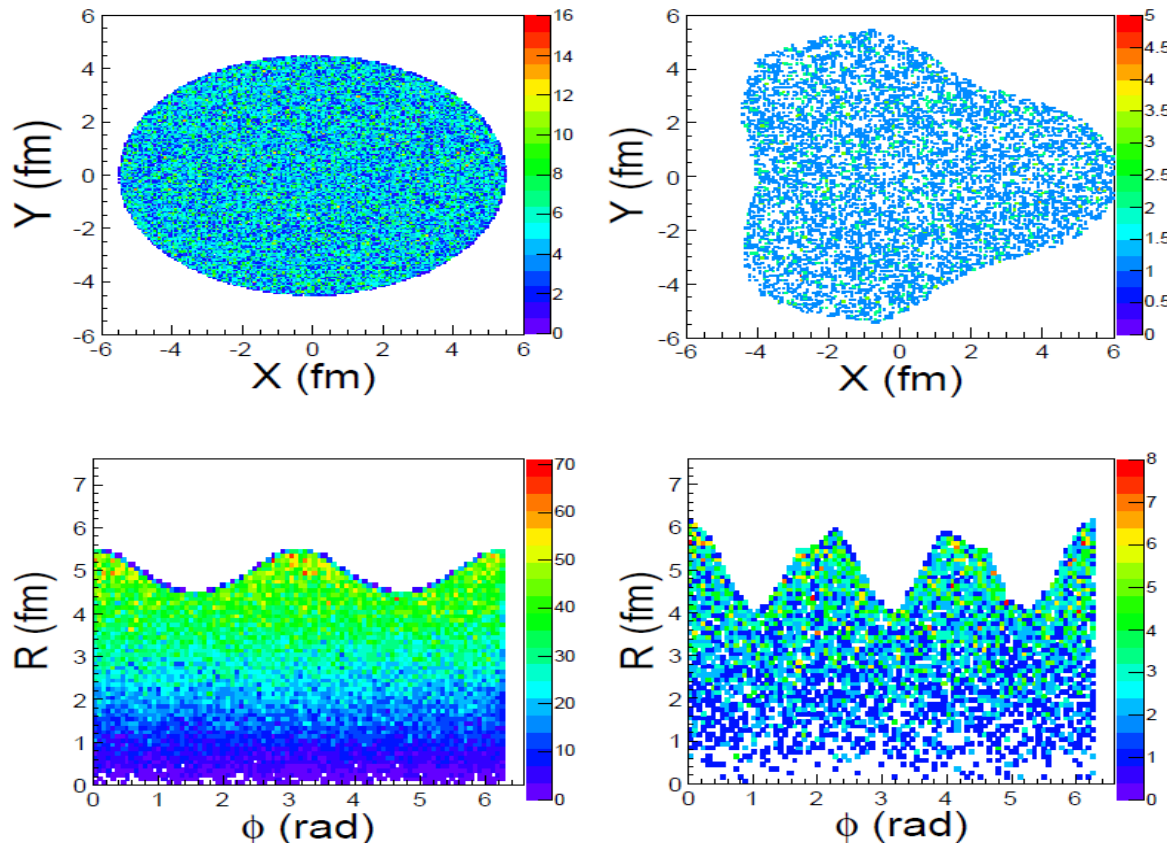
Hard part:

Parton energy loss depends on the path length in the medium: $v_2(\text{jet}) \neq 0$

HYDJET++: triangular flow

Space modulation of the freeze-out surface with independent phase Ψ_3 and parameter ϵ_3 is introduced in the model:

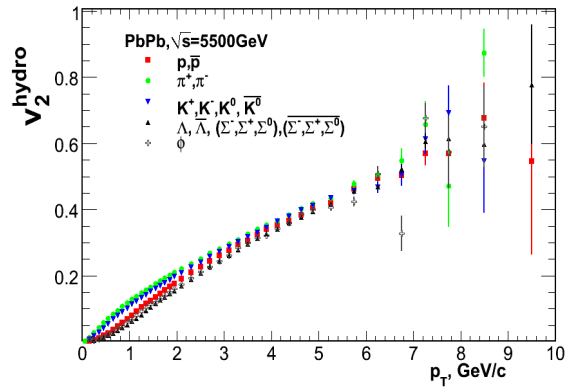
$$R(b, \phi) = R_f(b) \frac{\sqrt{1 - \epsilon^2(b)}}{\sqrt{1 + \epsilon(b) \cos 2\phi}} [1 + \epsilon_3(b) \cos 3(\phi + \Psi_3^{\text{RP}})] \quad \Psi_3 \neq \Psi_2$$



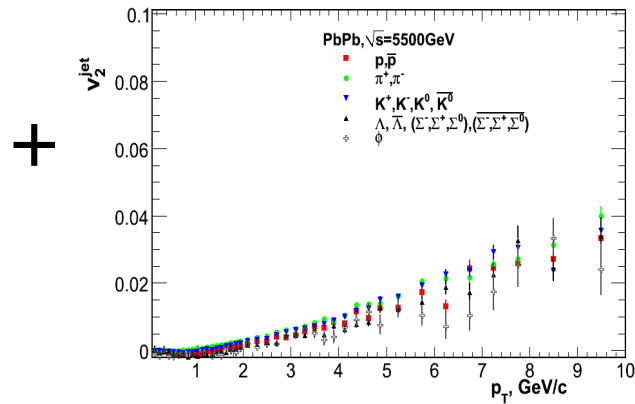
Particle densities in the transverse plane for v_2 and $v_2 + v_3$ harmonics.

HYDJET++ model: flow

Hydrodynamics

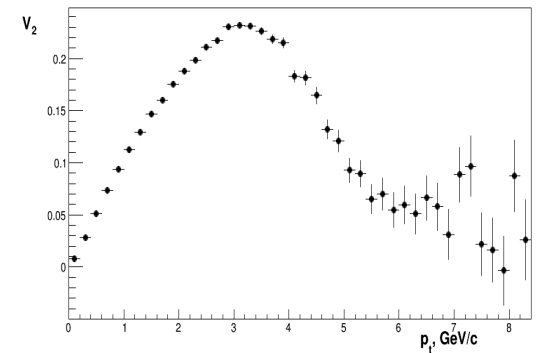


Jet part +quenching



+

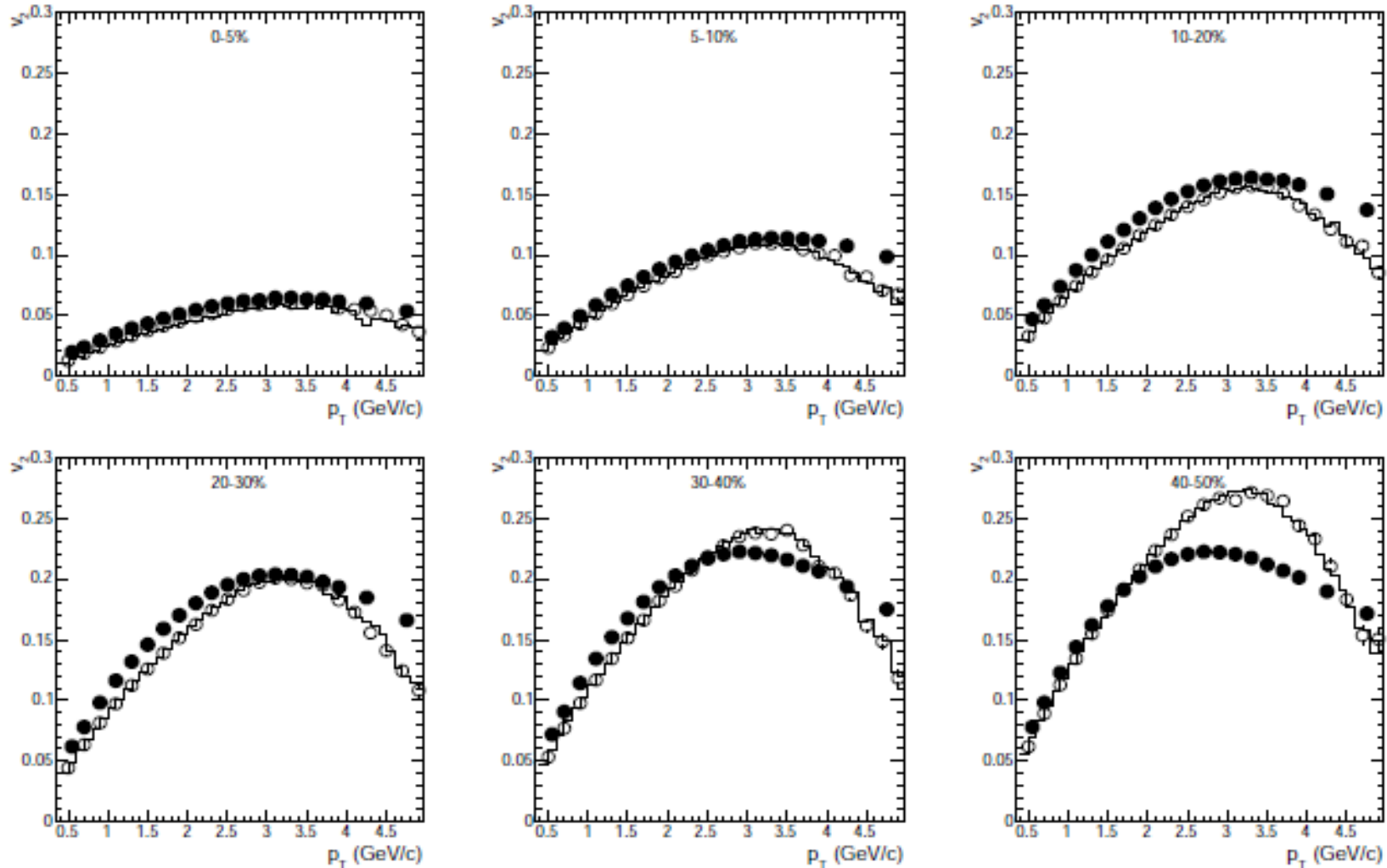
Typical flow pattern



- Even v_n appear in the model because of v_2
- Odd v_n appear in the model because of v_3

HYDJET++ : elliptic flow

V_2

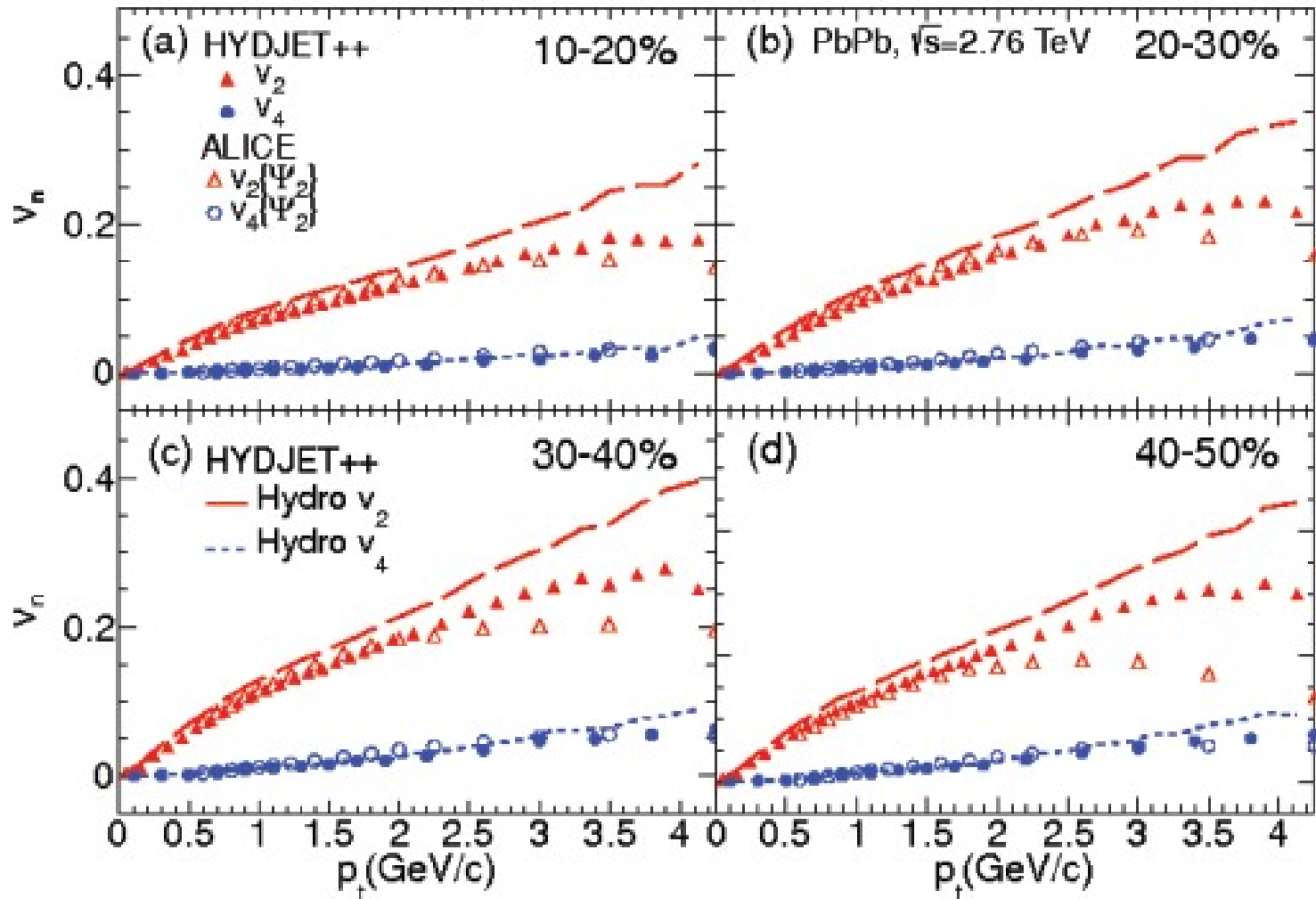


The closed circles: ATLAS data (Phys.Rev. C 86, (2012) 014907), $v_n\{EP\}$, PbPb collisions, 2.76 TeV,
open circles: $v_n\{EP\}$ for HYDJET++ , histograms: $v_n\{\Psi_{RP}\}$ for HYDJET++

Discrepancy in an intermediate p_T region.

HYDJET++ :

elliptic and quadrangular flow



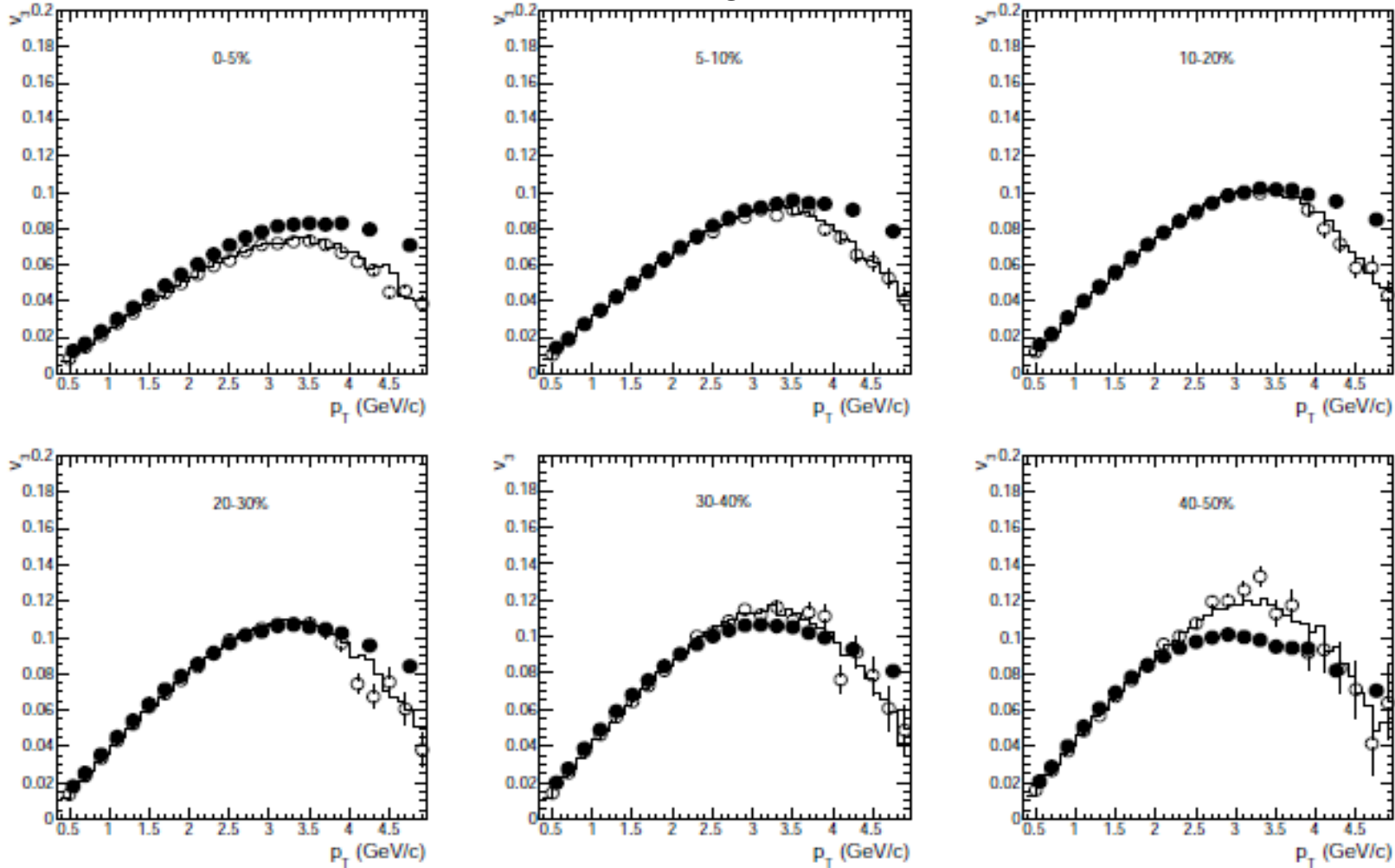
v_4 arising from v_2 (w.r.t Ψ_2) is described well.

In order to describe $v_4\{\Psi_4\}$ additional modulation of flow velocity is introduced currently, no independent Ψ_4 .

HYDJET++ : triangular flow

The simple parametrization: $v_3(b) \propto \epsilon_0^{1/3}(b)$

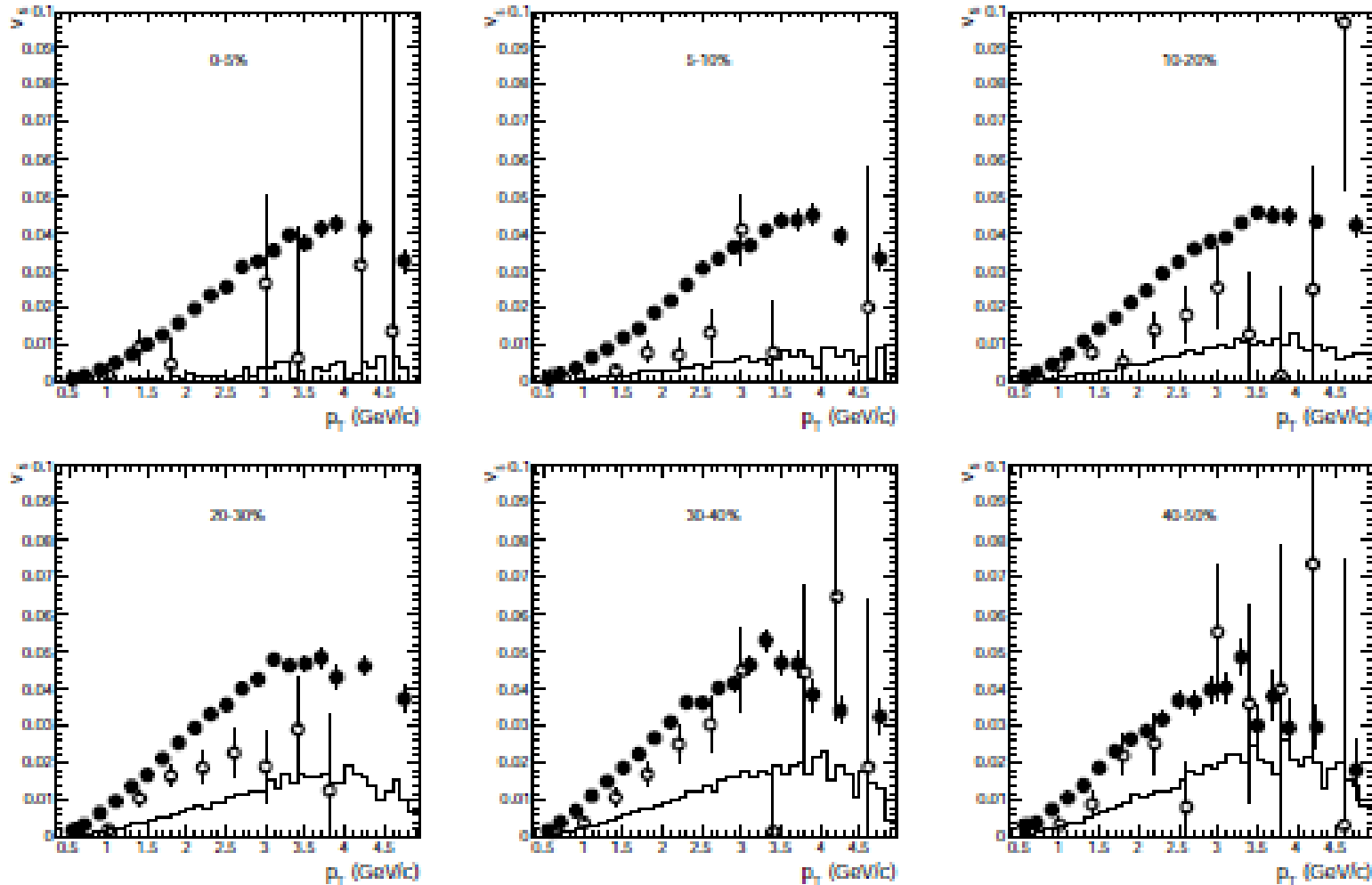
V_3



The closed circles: ATLAS data (Phys.Rev. C 86, (2012) 014907), $v_n\{EP\}$, PbPb collisions, 2.76 TeV,
open circles: $v_n\{EP\}$ for HYDJET++, histograms: $v_n(\Psi_{RP})$ for HYDJET++

HYDJET++ : higher order harmonics

V_5

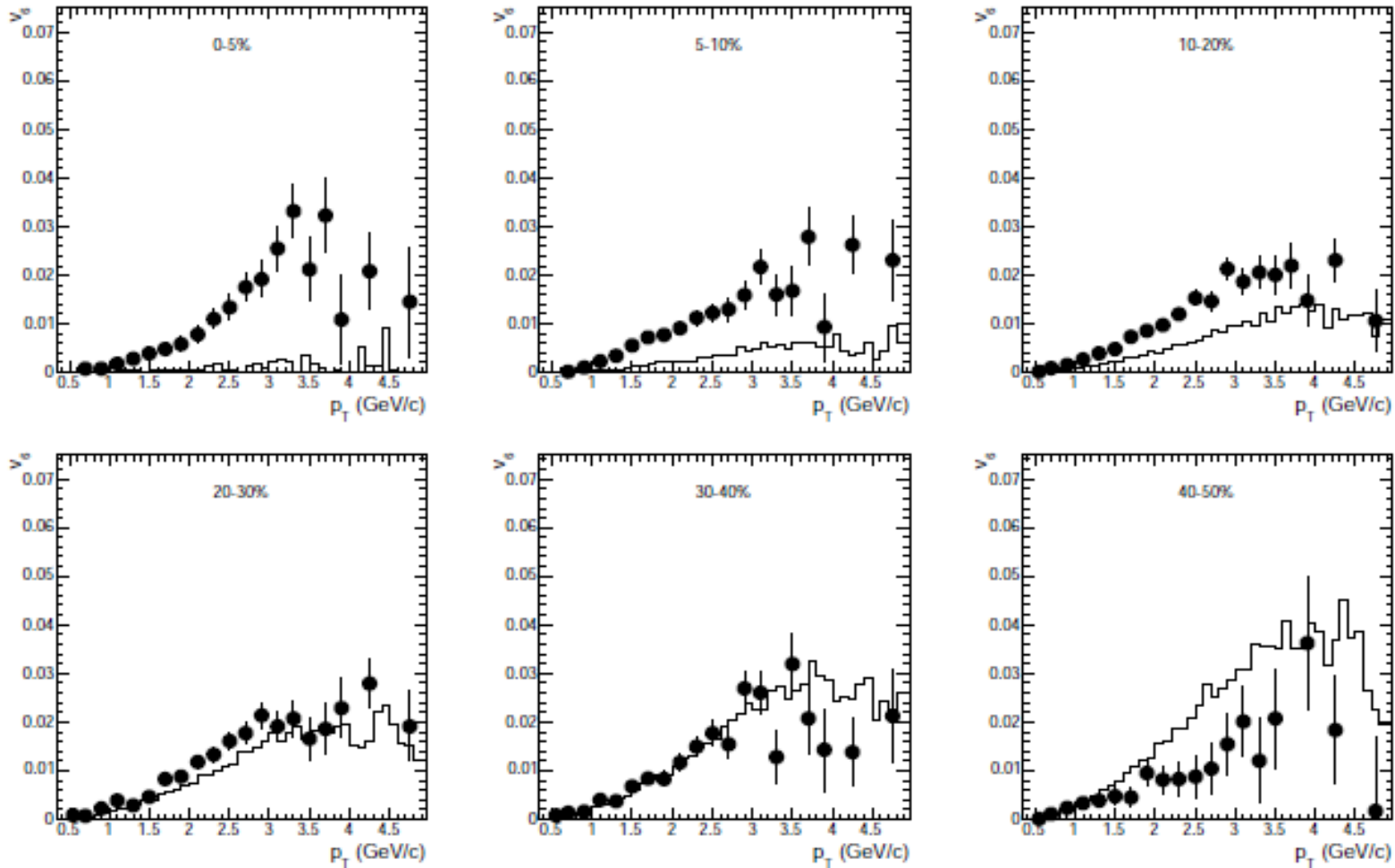


The closed circles: CMS data $v_n\{EP\}$, PbPb collisions, 2.76 TeV,
open circles: $v_n\{EP\}$ for HYDJET++ ; histograms: $v_n(\Psi_{RP})$ for HYDJET++

central collisions → the possible presence of the additional pentagonal flow parameter

HYDJET++ : higher order harmonics

V_6

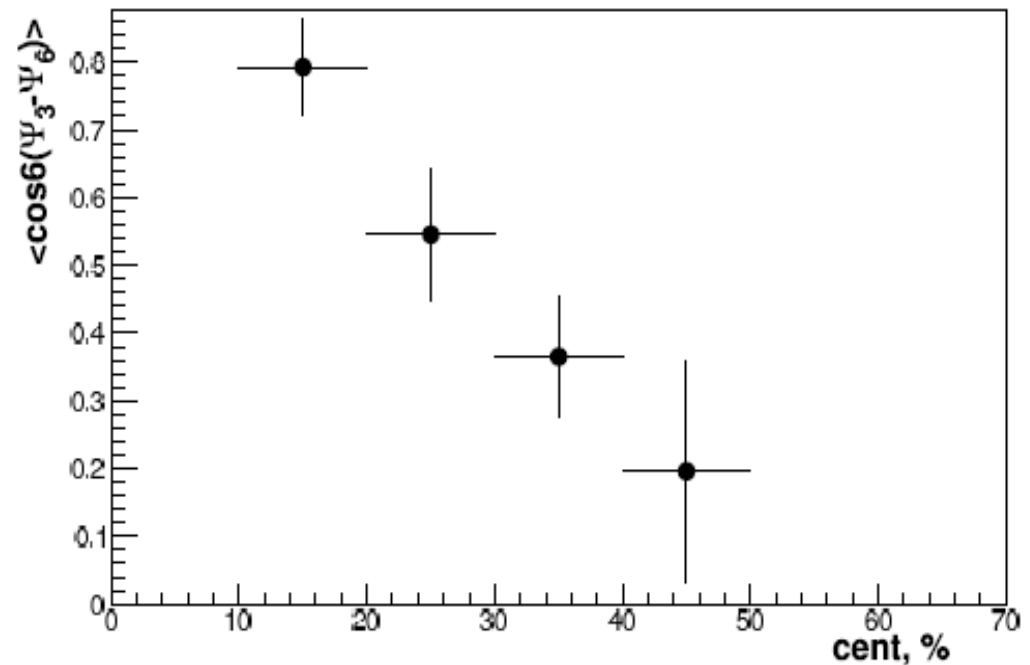
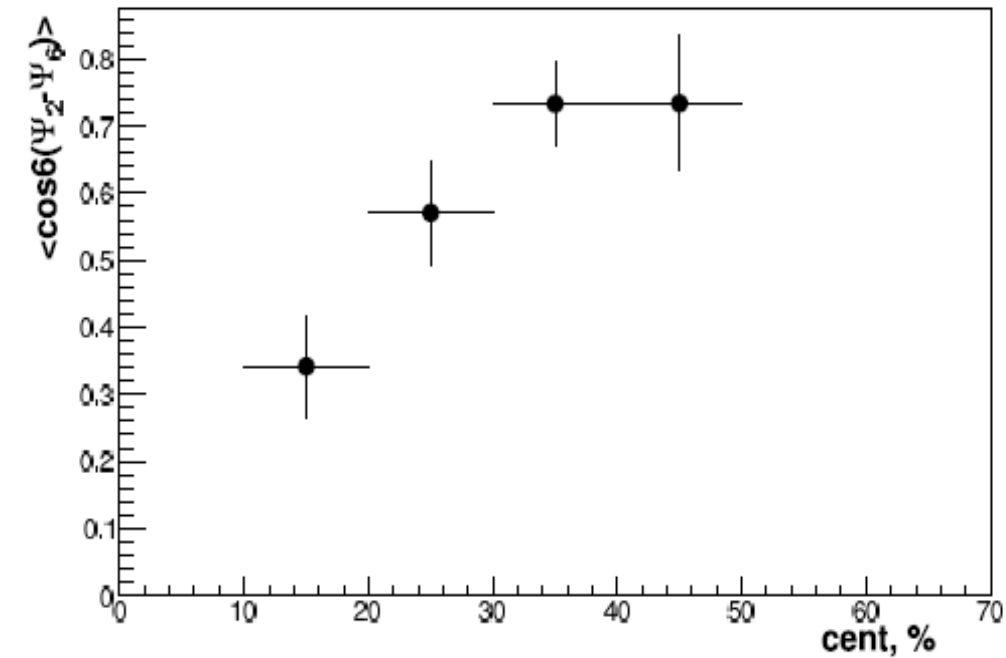


The closed circles: CMS data $v_6\{\text{EP}\}$, PbPb collisions, 2.76 TeV,
histograms: $v_6(\Psi_2)$ for HYDJET++ ; $v_6(\Psi_6)$ in progress

V_6 also has a contribution from v_3 (only contribution from v_2 is shown).

Two-plane correlators

Ψ_2, Ψ_3 are known in the model, Ψ_6 is reconstructed with EP method.



Contribution from v_3 increases for more central collisions.

Behavior of the plane correlators is in line with the experimental observations.

Dihadron angular triggered correlations

Signal: correlations of a pair in the same event:

$$S(\Delta\varphi, \Delta\eta) = \frac{1}{N_{trig}} \frac{d^2 N^{same}}{d\Delta\varphi d\Delta\eta}$$

Background: correlations of two particles from different events:

$$B(\Delta\varphi, \Delta\eta) = \frac{1}{N_{trig}} \frac{d^2 N^{mixed}}{d\Delta\varphi d\Delta\eta}$$

Correlation function, definition 1

$$C(\Delta\phi, \Delta\eta) \equiv \frac{N_{mixed}}{N_{same}} \times \frac{N_{same}(\Delta\phi, \Delta\eta)}{N_{mixed}(\Delta\phi, \Delta\eta)}$$

definition 2

$$\frac{1}{N_{trig}} \frac{d^2 N}{d\Delta\varphi d\Delta\eta} = B(0,0) \frac{S(\Delta\varphi, \Delta\eta)}{B(\Delta\varphi, \Delta\eta)}$$

$$\Delta\varphi = \varphi_1 - \varphi_2$$

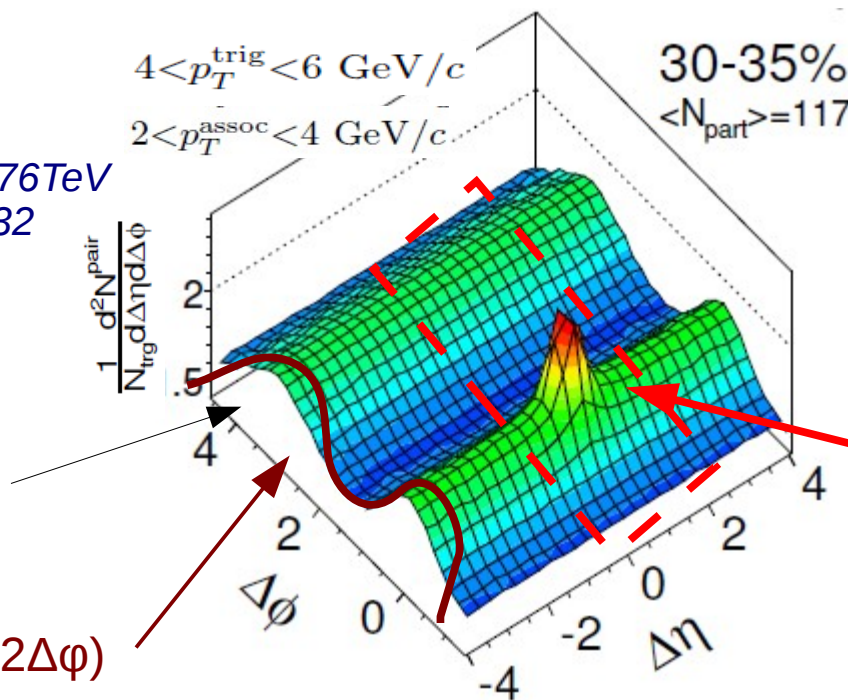
$$\Delta\eta = \eta_1 - \eta_2$$

N_{trig} : number of trigger particles.

CMS, PbPb 2.76TeV
arXiv:1107.0032

Away-side peak from jet is broad on $\Delta\eta$

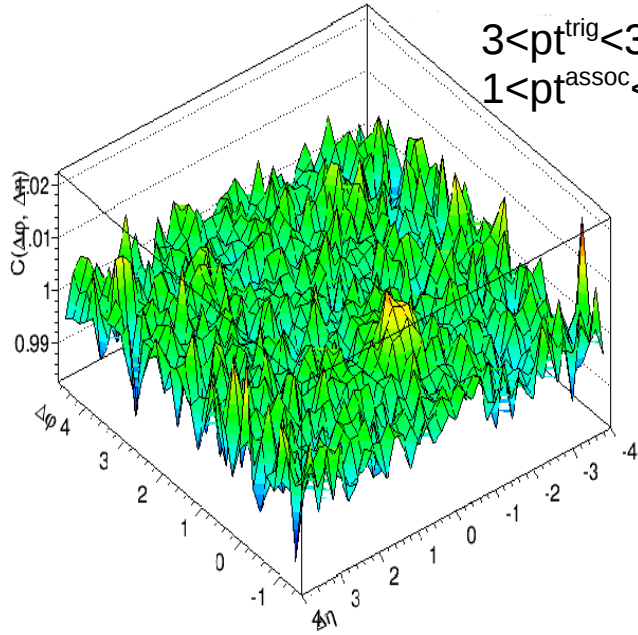
Flow, $\cos(2\Delta\varphi)$



Short range correlations (small $\Delta\eta$): hadrons inside jets, clusters, resonances

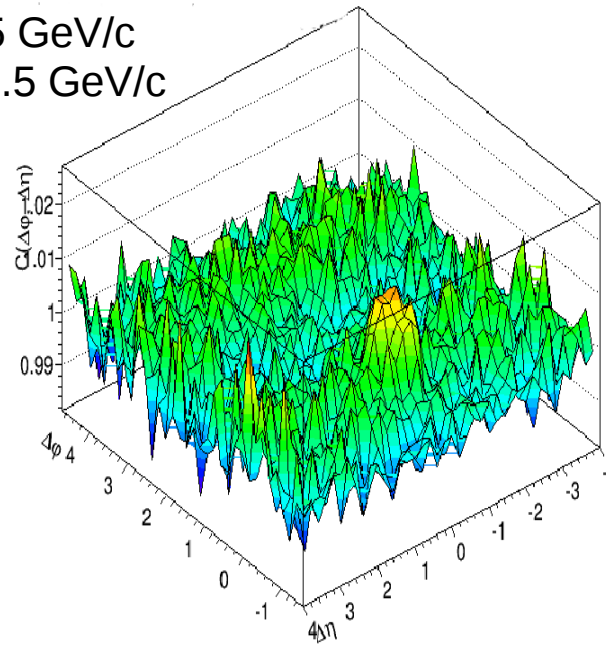
Dihadron angular correlation in HYDJET++, PbPb 2.76 TeV

0% centrality

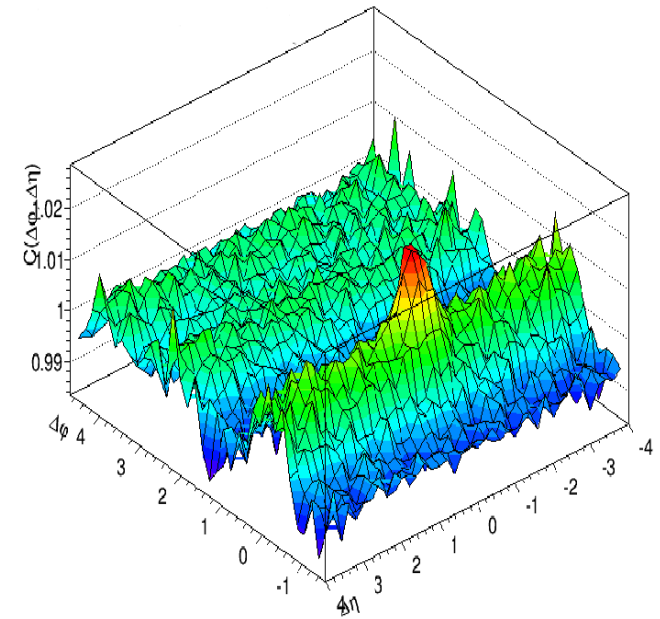


$3 < p_t^{\text{trig}} < 3.5 \text{ GeV}/c$
 $1 < p_t^{\text{assoc}} < 1.5 \text{ GeV}/c$

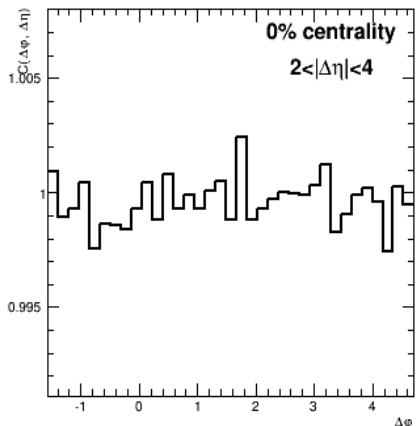
0-5% centrality, v_2 only



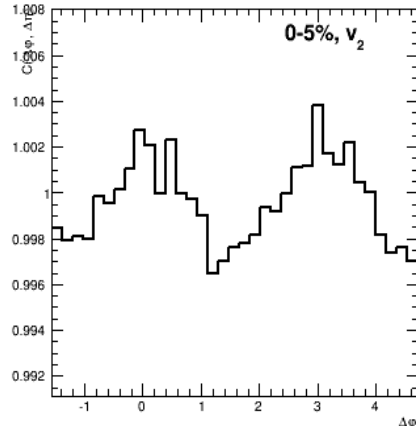
0-5% centrality, v_2 & v_3



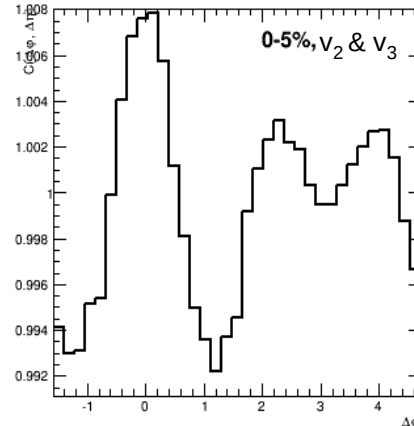
Ridge region, 1D



0% centrality
 $2 < |\Delta\eta| < 4$



0-5%, v_2

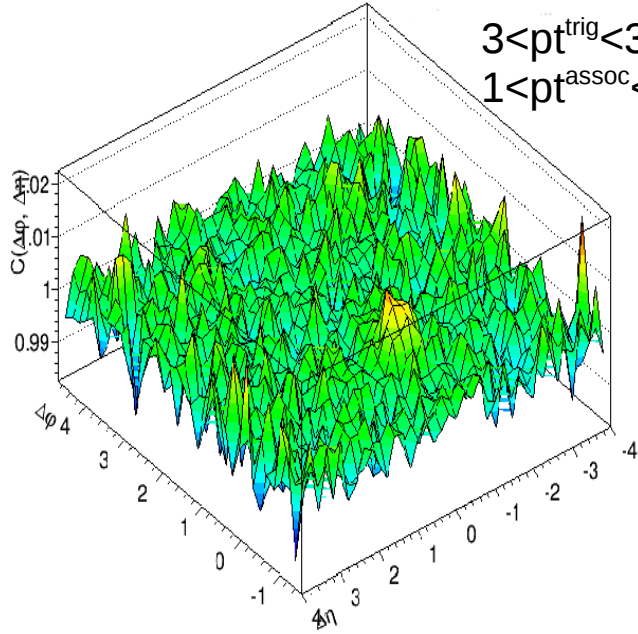


0-5%, v_2 & v_3

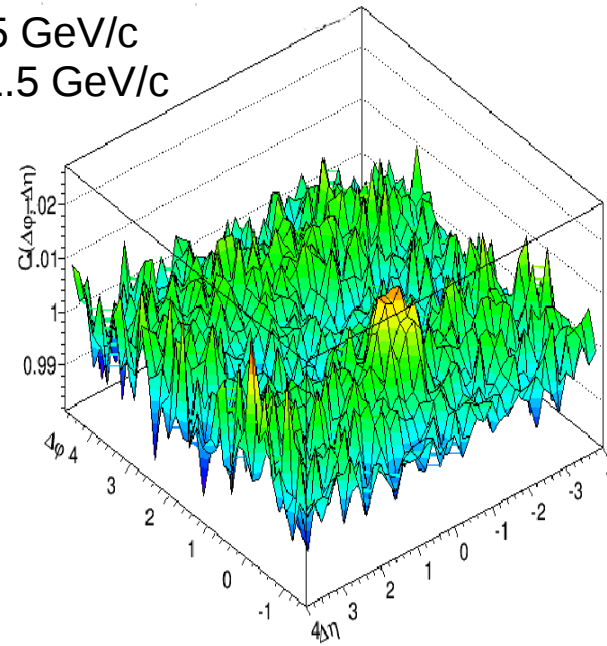
- The ridge effect appears in the model because of flow v_2 and v_3
- v_3 leads to double-peak structure at away-side on $\Delta\phi$

Dihadron angular correlation in HYDJET++, PbPb 2.76 TeV

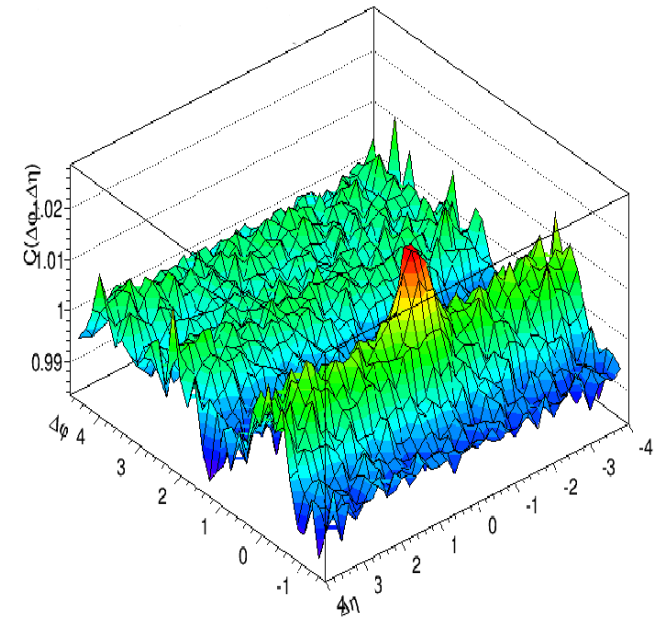
0% centrality



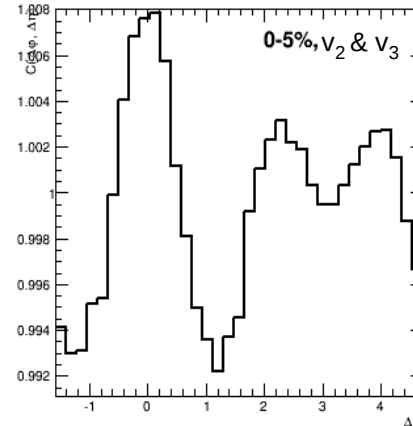
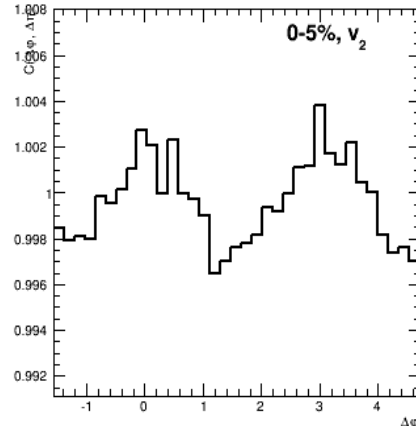
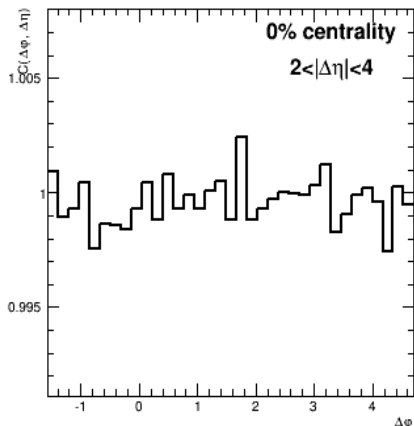
0-5% centrality, v_2 only



0-5% centrality, v_2 & v_3



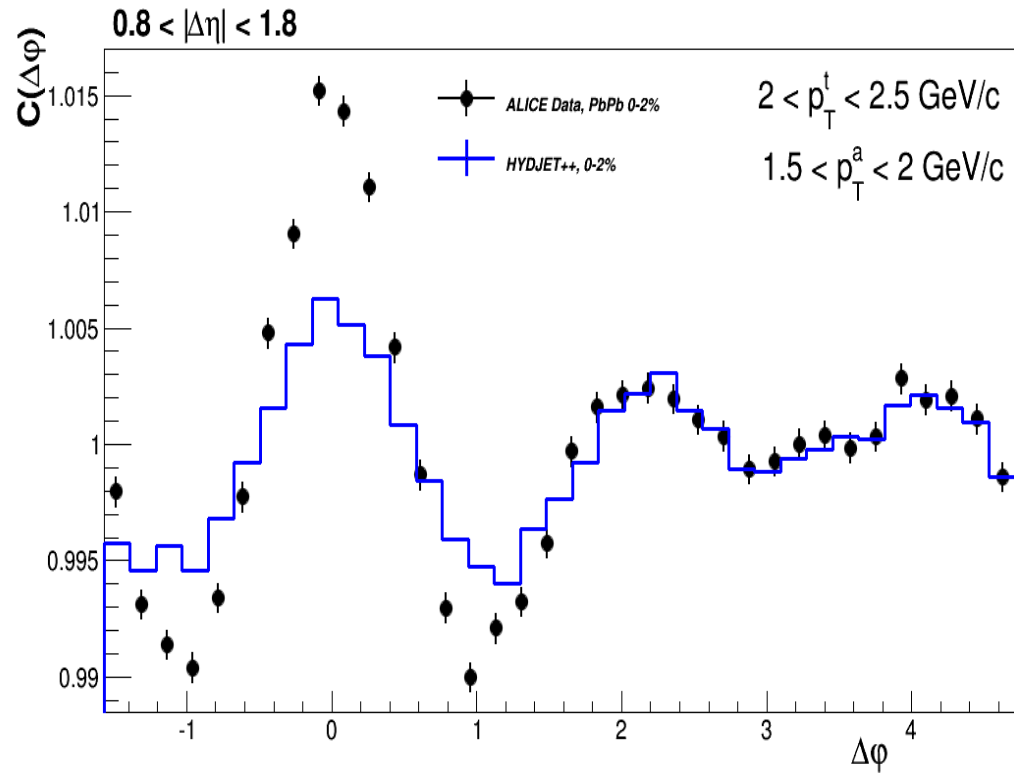
Ridge region, 1D



- The ridge effect appears in the model because of flow v_2 and v_3
- v_3 leads to double-peak structure at away-side on $\Delta\phi$

HYDJET++ data comparison

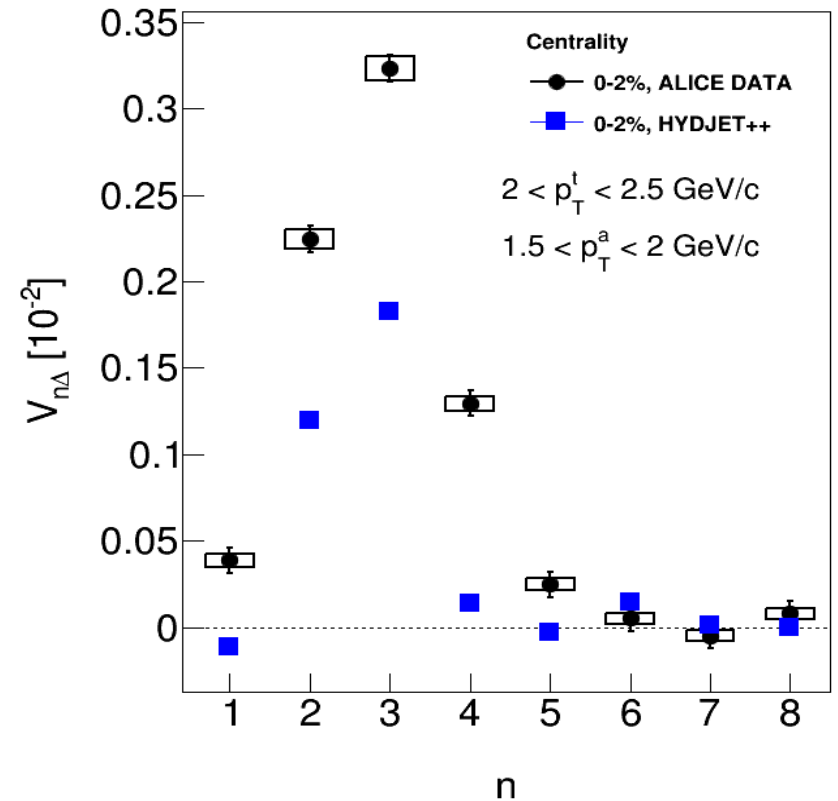
Ultra-central collisions, 0-2%



DATA: *PLB 708, 249 (2012) ALICE*

- The ridge is smaller than in data
- Away-side structure is described well

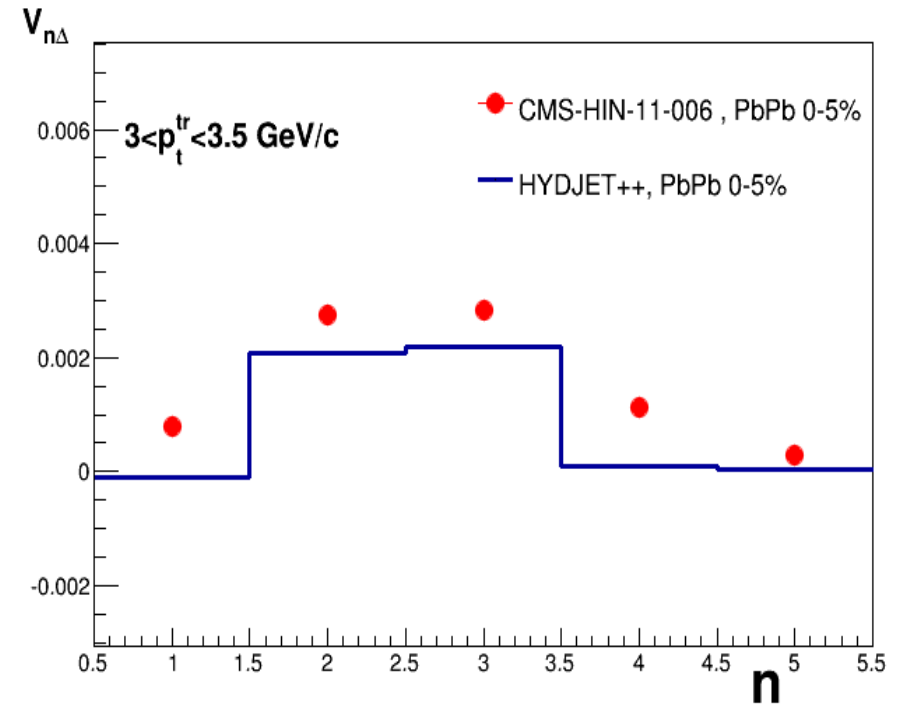
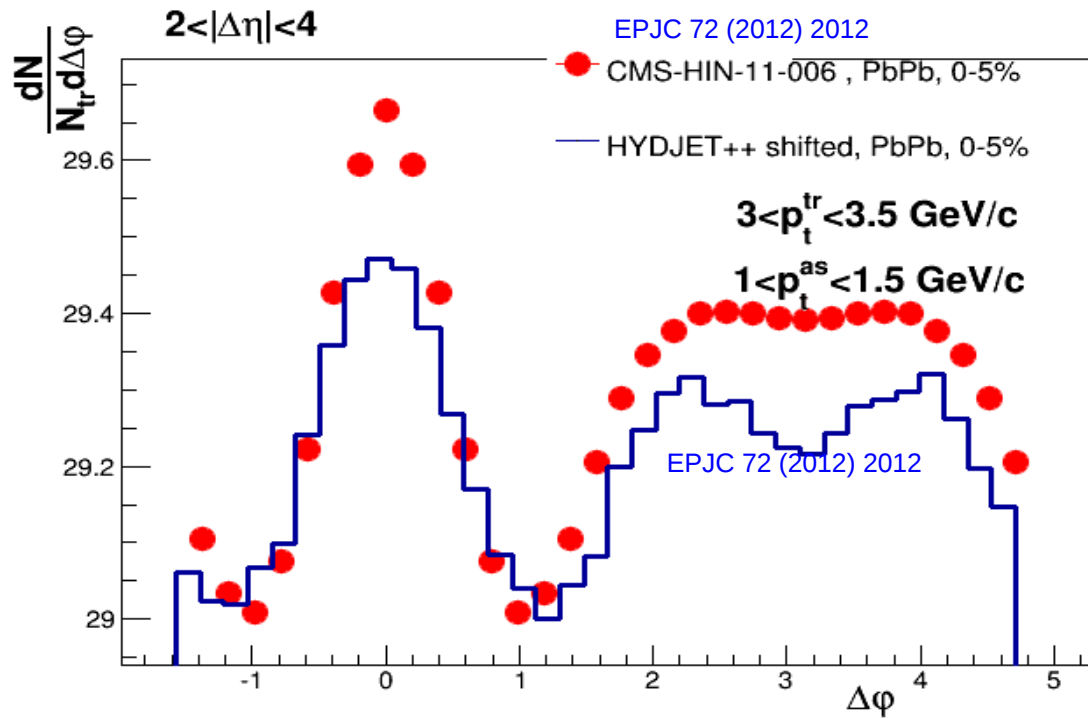
$$\frac{dN^{\text{pairs}}}{d\Delta\phi} \propto 1 + \sum_{n=1}^{\infty} 2V_{n\Delta}(p_T^t, p_T^a) \cos(n\Delta\phi)$$



- Coefficients $V_{\Delta 2}$, $V_{\Delta 3}$ are smaller and $V_{\Delta 4}$, $V_{\Delta 5}$ are negligible compared to data

HYDJET++ data comparison

Central collisions, 0-5%

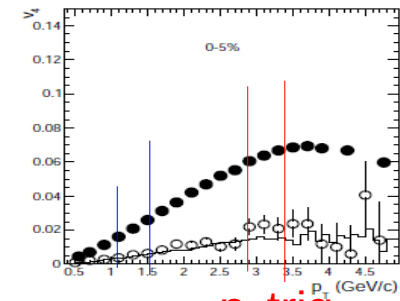
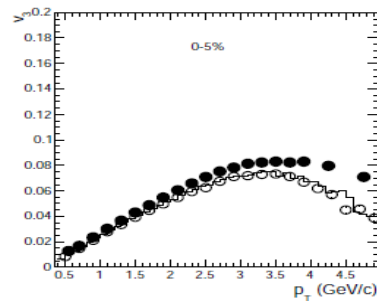
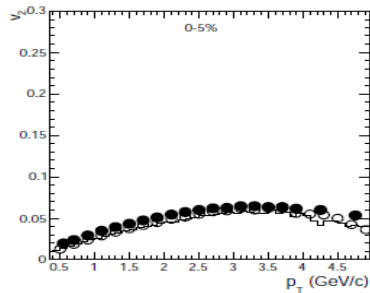


Singular particle flow:

V_2

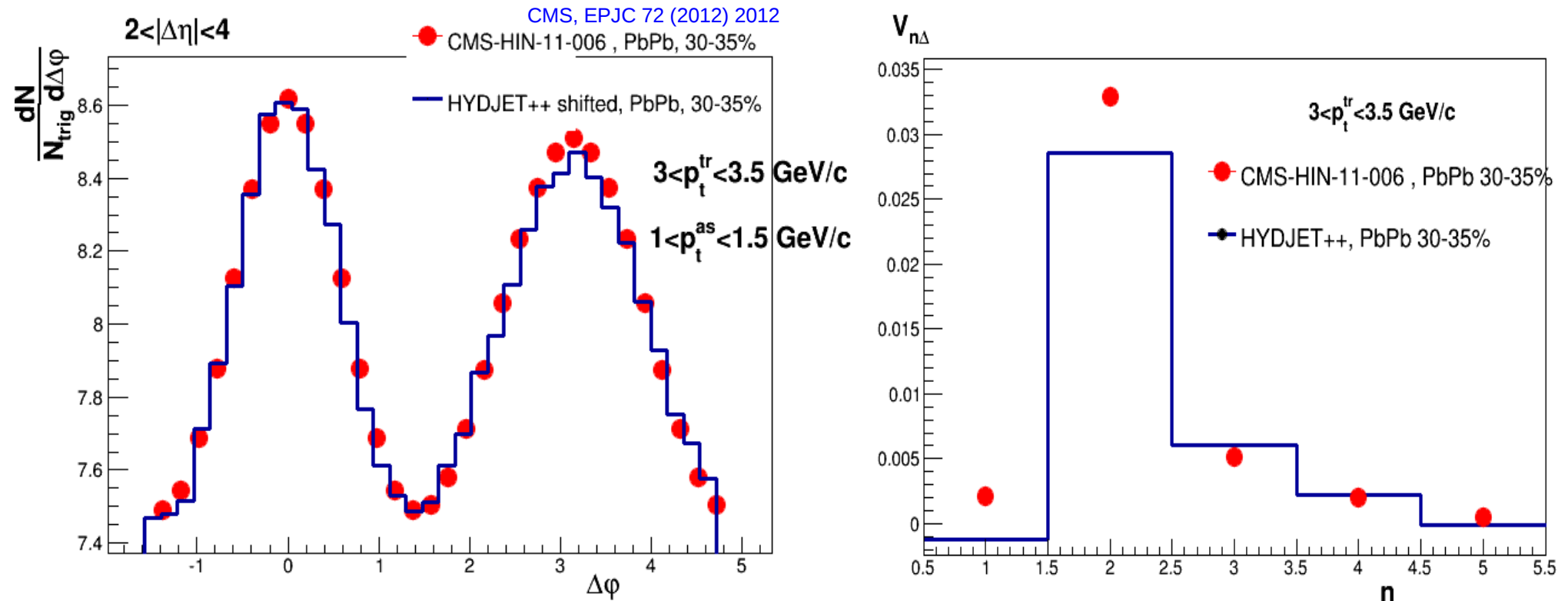
V_3

V_4



HYDJET++ data comparison

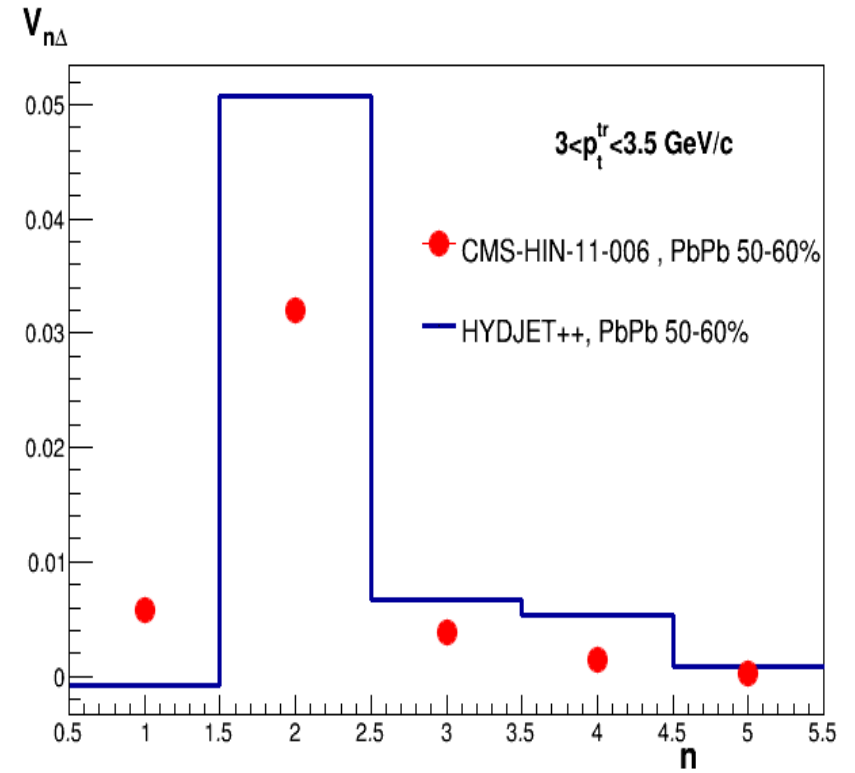
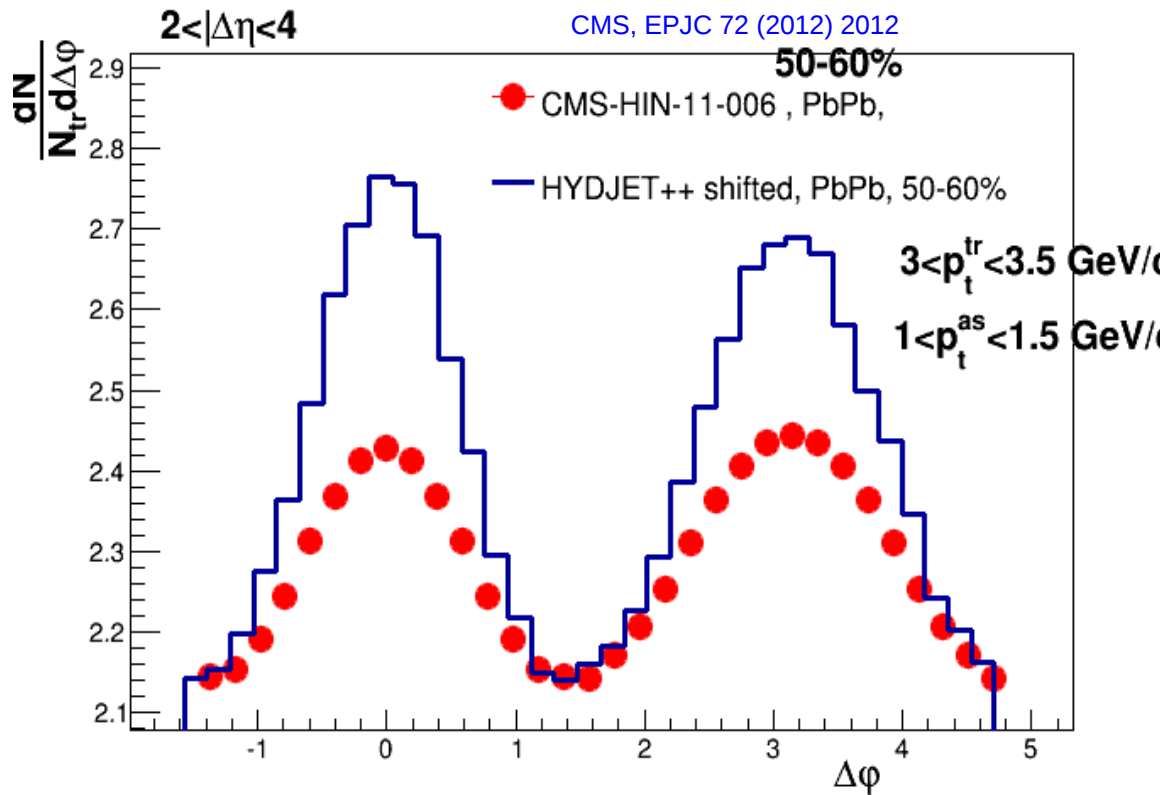
Mid-central collisions, 30-35%



Singular particle flows are described well in this region.

HYDJET++ data comparison

More peripheral collisions, 50-60%



Coefficients $V_{\Delta 2}$ is much smaller compared to data.

HYDJET++

data comparison, momentum dependence

Central collisions, 0-5%

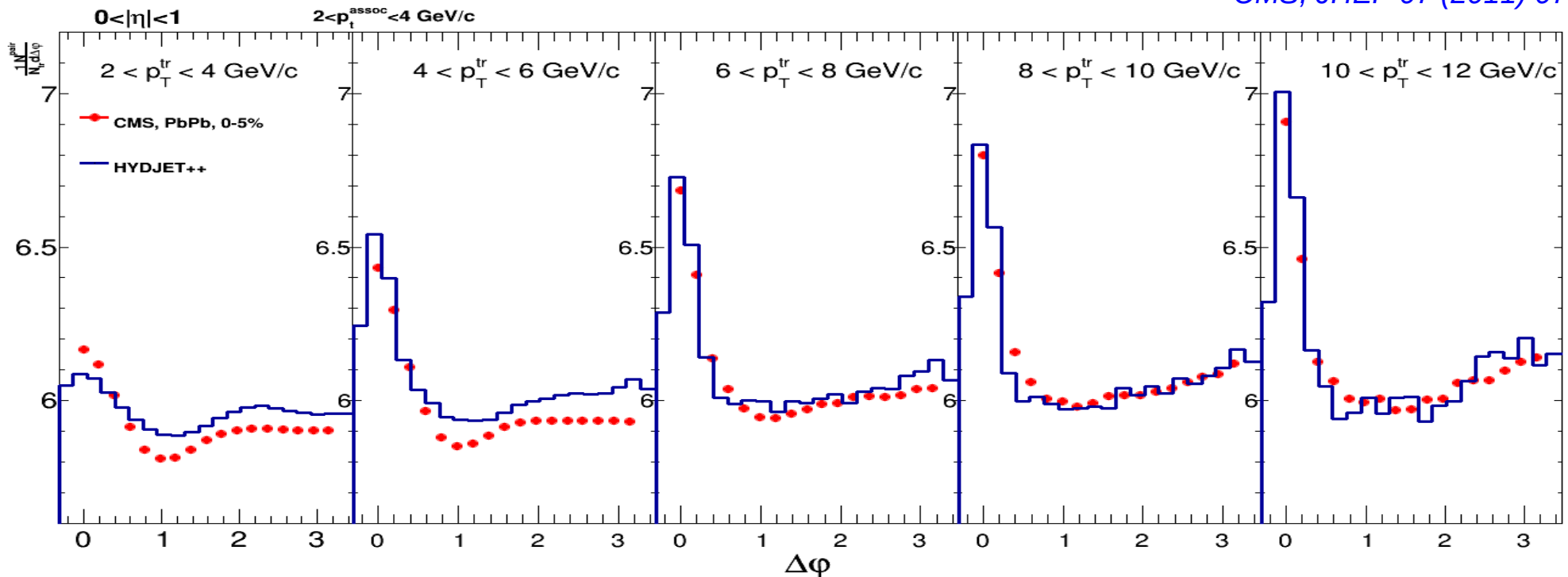
Short range correlations, $|\Delta\eta| < 1$

flow+non-flow

p_t^{tr}

non-flow (jets)+jet quenching

CMS, JHEP 07 (2011) 076

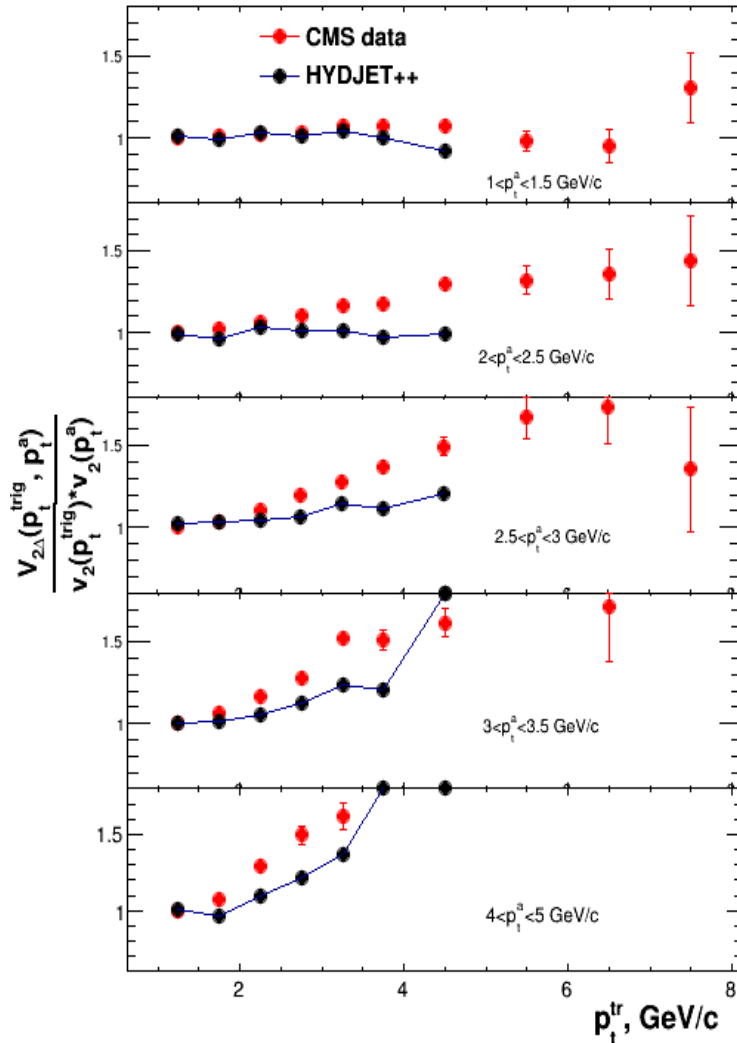


- At 0-5% centrality, HYDJET++ does not reproduce flow harmonics v_n ($n > 2$) very well, neither it reproduces dihadron correlations at low p_t^{tr} .
- At high p_t^{tr} HYDJET++ describes data.

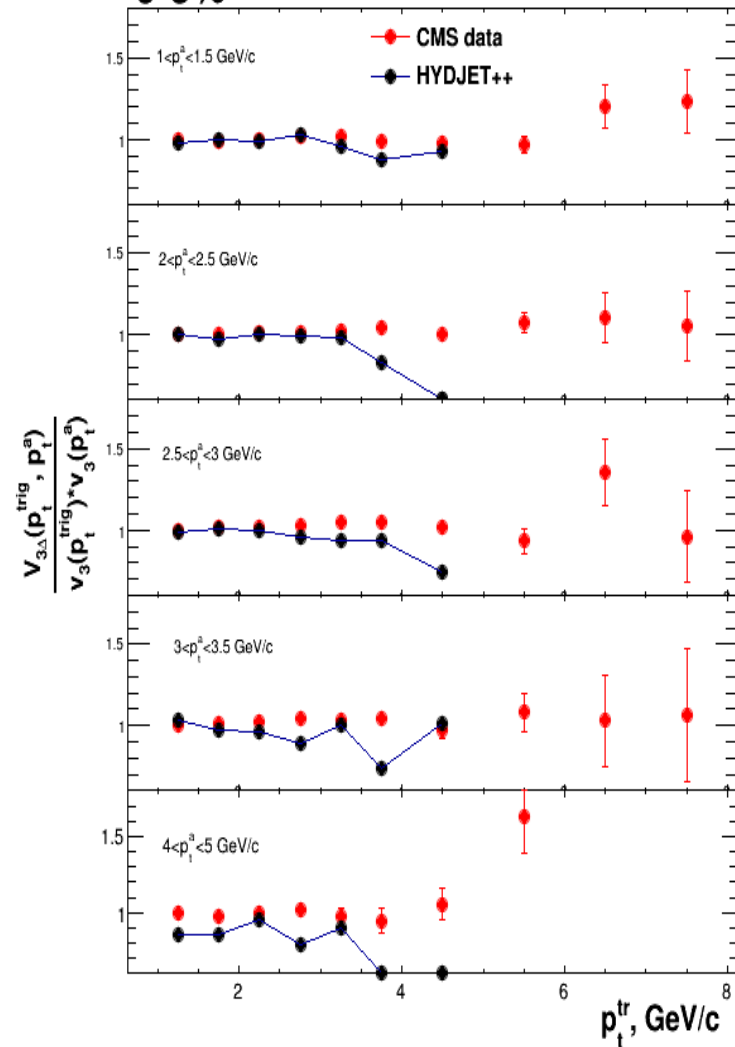
Test of factorization: $V_{\Delta n} \approx v_n\{2\}(p_t^{\text{tr}}) * v_n\{2\}(p_t^{\text{a}})$

At low p_t one neglects non-flow and estimates: $v_n(p_t^{\text{low}}) = \sqrt{V_{\Delta n}(p_t^{\text{low}}, p_t^{\text{low}})}$; $v_n(p_t) = V_{\Delta n}(p_t, p_t^{\text{low}}) / v_n(p_t^{\text{low}})$

$V_{\Delta 2}$ factorization



0-5%



$V_{\Delta 3}$ factorization

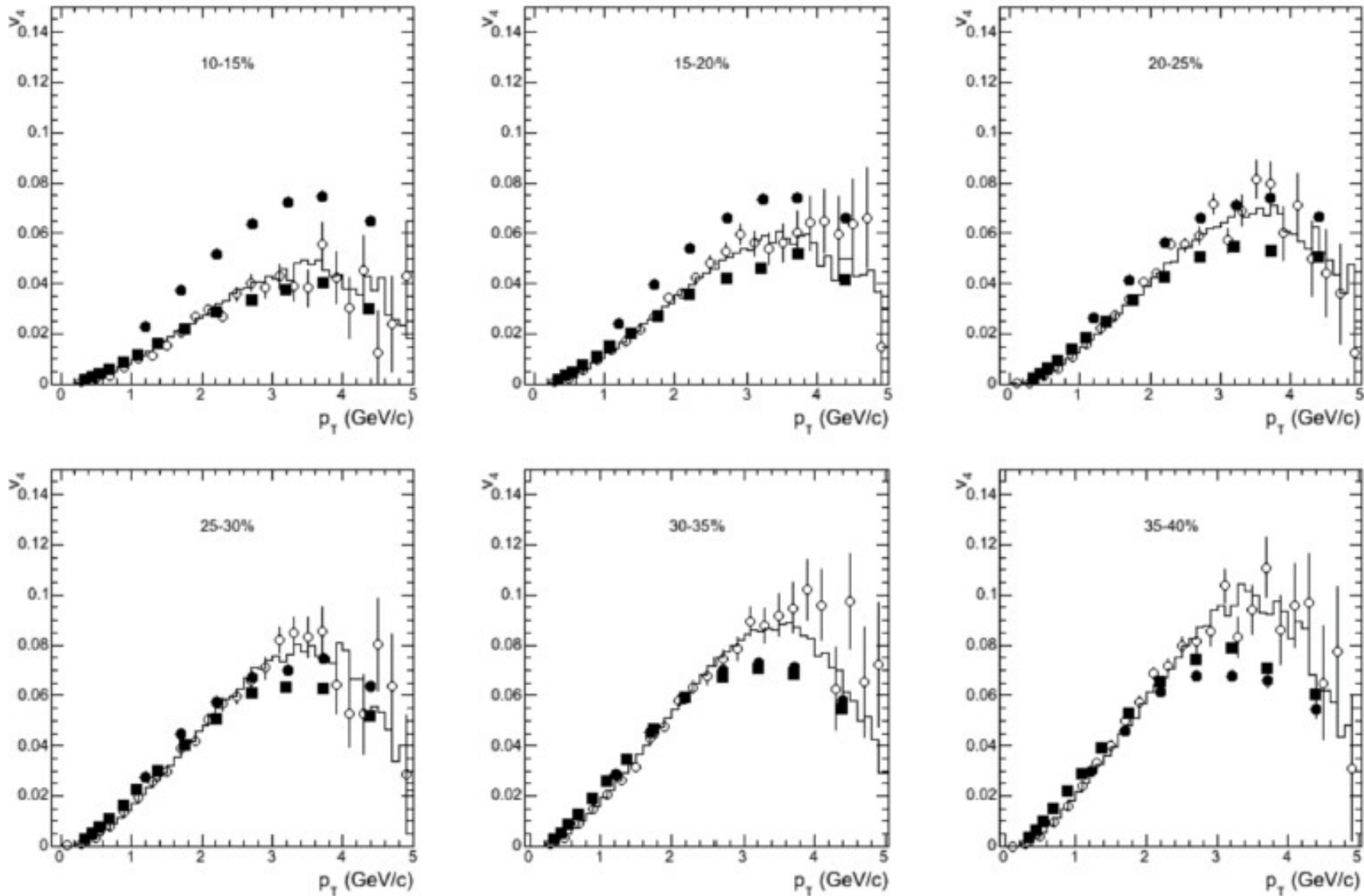
- Factorization in HYDJET++ breaks due to hard component (non-flow).
- Factorization for $V_{\Delta 2}$ breaks in data at lower p_t compared to HYDJET++.

Conclusion

- Flow in the model:
 - Uncorrelated EbE reaction planes Ψ_2 and Ψ_3 are introduced, independent on η and p_t .
 - Multiplicity fluctuation at the same impact parameter \rightarrow flow v_2 and v_3 fluctuations (no additional fluctuations due to eccentricity fluctuations)
 - Higher flow harmonics appear from v_2 and v_3 interference in final state (at freeze-out)
- Data on higher flow harmonics and dihadron angular correlations are described well in mid-central collisions
- The mechanism of interference of v_2 and v_3 is not enough to describe data in central collisions

Backups

HYDJET++ : quadrangular flow

 V_4 

CMS data, $v_4\{2\}$ — circles, $v_4\{LYZ\}$ — squares

L. Bravina et al., Eur. Phys. J C 74 (2014) 2807

Correlation pattern in AA

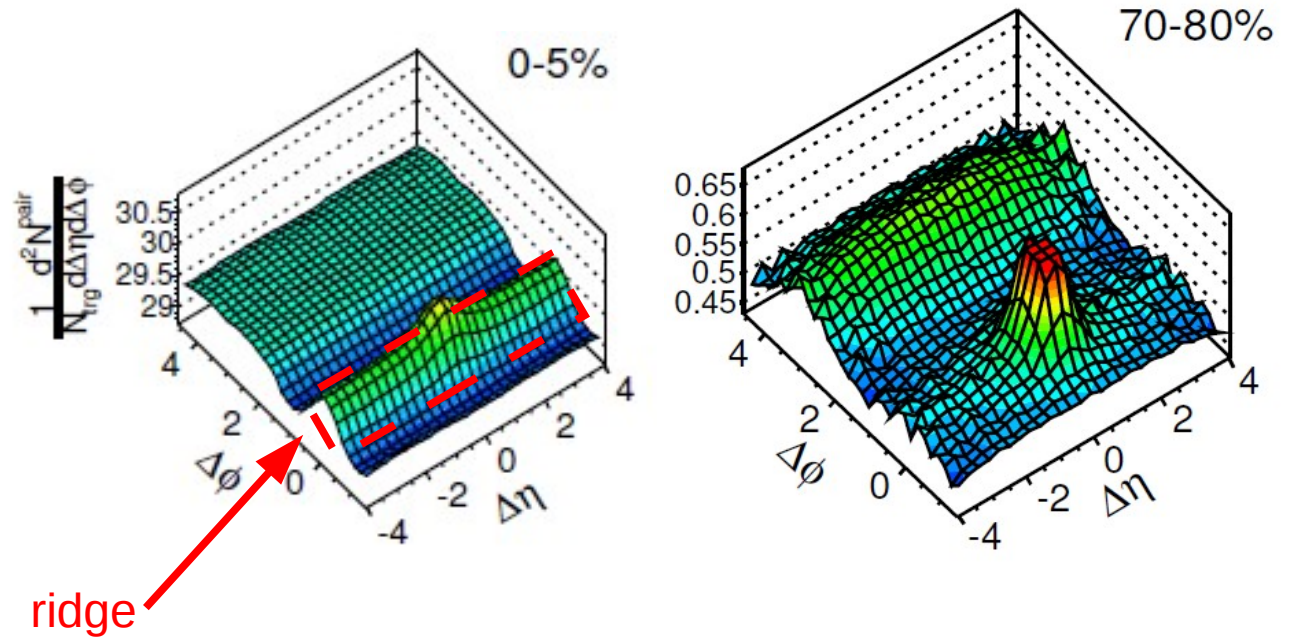
CMS, PbPb 2.76 TeV, Eur. Phys. C 72 (2012) 10052, $3 < p_{t}^{\text{trig}} < 3.5 \text{ GeV}/c$, $1 < p_{t}^{\text{assoc}} < 1.5 \text{ GeV}/c$

Central collisions:

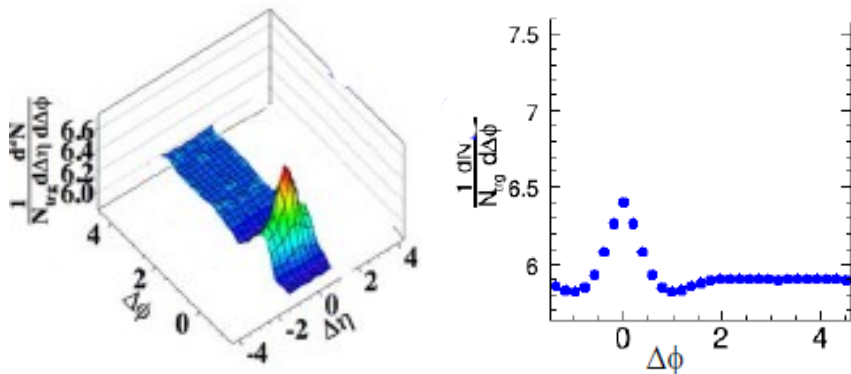
- The back jet is quenched
- Small flow v_2
- ridge

Peripheral collisions:

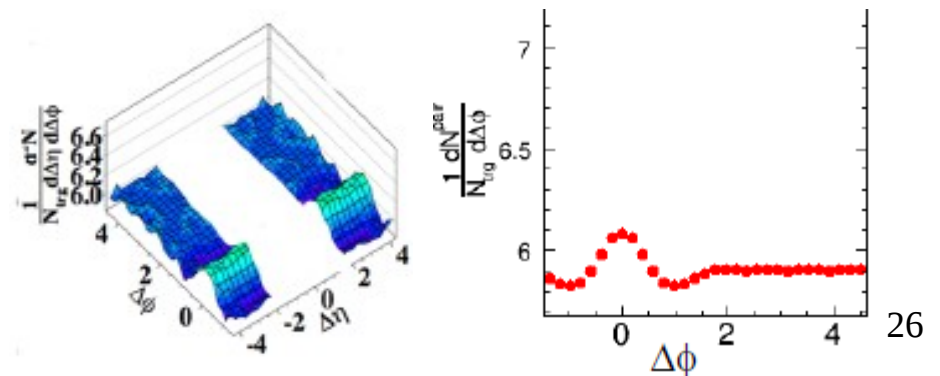
- Back jet peak
- Small flow v_2
- Small ridge



Jet region, 2D vs 1D



Ridge region



HYDJET++, hard component

Parton collisional loss (high momentum transfer approximation)

$$\frac{dE^{col}}{dl} = \frac{1}{4T\lambda\sigma} \int_{\mu_D^2}^{t_{max}} dt \frac{d\sigma}{dt} t \quad \frac{d\sigma}{dt} \simeq C \frac{2\pi\alpha_s^2(t)}{t^2} \frac{E^2}{E^2 - m_p^2}, \quad \alpha_s = \frac{12\pi}{(33 - 2N_f) \ln(t/\Lambda_{QCD}^2)}$$

t is momentum transfer, E and m_p : energy and mass of a hard parton, C is color factor

Radiative loss (coherent gluon radiation in Baier-Dokshitzer-Mueller-Schiff formalism)

– *For massless parton*

$$\frac{dE^{rad}}{dl} = \frac{2\alpha_s(\mu_D^2)C_R}{\pi L} \int_{\omega_{min}}^E d\omega \left[1 - y + \frac{y^2}{2} \right] \ln |\cos(\omega_1\tau_1)| \quad \omega_1 = \sqrt{i \left(1 - y + \frac{C_R}{3}y^2 \right) \bar{\kappa} \ln \frac{16}{\bar{\kappa}}} \quad \text{with} \quad \bar{\kappa} = \frac{\mu_D^2 \lambda_g}{\omega(1-y)} \quad \tau_1 = L/(2\lambda_g), \quad y = \omega/E$$

ω is gluon energy

– *For heavy quark (dead cone approximation)*

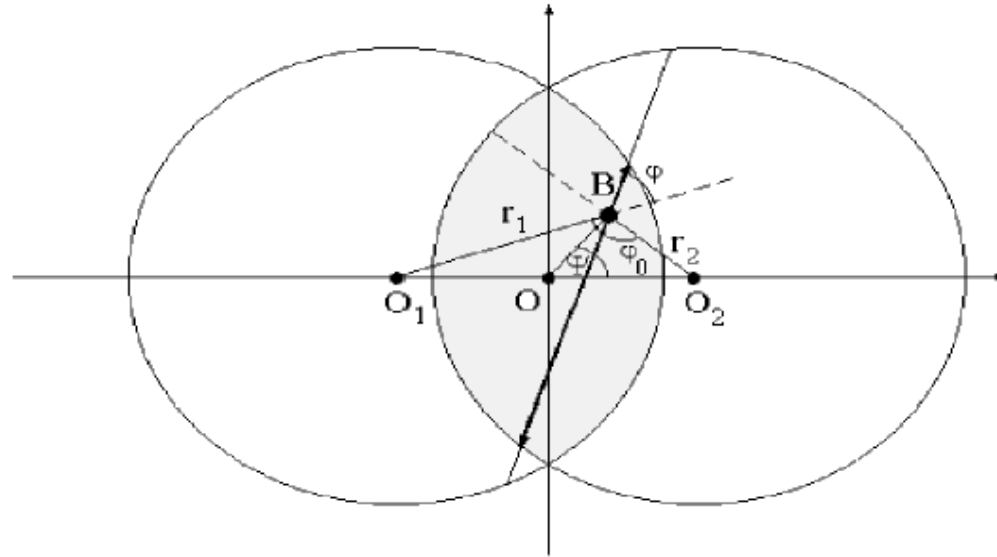
$$\frac{dE}{dl d\omega} \Big|_{m_q \neq 0} = \frac{1}{(1 + (\beta\omega)^{3/2})^2} \frac{dE}{dl d\omega} \Big|_{m_q = 0}, \quad \beta = \left(\frac{\lambda}{\mu_D^2} \right)^{1/3} \left(\frac{m_q}{E} \right)^{4/3}$$

HYDJET++, hard component

Geometry of QGP

Radial profile of energy density

$$\varepsilon(r_1, r_2) \propto T_A(r_1) * T_A(r_2) \quad (T_A(b) - \text{nuclear thickness function})$$



Jet production vertexes distribution:

$$\frac{dN^{\text{jet}}}{d\psi r dr}(b) = \frac{T_A(r_1) \cdot T_A(r_2)}{T_{AA}(b)}$$

HYDJET++, hard component

Halting the rescattering if:

(a) the parton escapes the hot QGP zone, i.e. the temperature in the next point $T(\tau_{i+1}, r_{i+1}, \eta_{i+1})$ becomes lower than T_c

(b) the parton loses so much of energy that its transverse momentum $p_T(\tau_{i+1})$ drops below the average transverse momentum of the “thermal” constituents of the medium.

Three model parameters: initial QGP temperature T_0 ,
QGP formation time τ_0 and
number of active quark flavors in QGP N_f
(+ minimal p_T of hard process P_{tmin})

HYDJET++, soft component

N.S.Amelin, R.Lednisky, T.A.Pocheptsov, I.P.Lokhtin, L.V.Malinina, A.M.Snigirev, Yu.A.Karpenko, Yu.M.Sinyukov, Phys. Rev. C 74 (2006) 064901

N.S.Amelin, R.Lednisky, I.P.Lokhtin, L.V.Malinina, A.M.Snigirev, Yu.A.Karpenko, Yu.M.Sinyukov, I.C.Arsene, L.Bravina, Phys. Rev. C 77 (2008) 014903

Starting point: chemical freeze-out of fireball with the distribution functions in the fluid element rest frame

$$f_i^{\text{eq}}(p^{*0}; T^{\text{ch}}, \mu_i, \gamma_s) = \frac{g_i}{\gamma_s^{-n_i^s} \exp([p^{*0} - \mu_i]/T^{\text{ch}}) \pm 1}$$

p^{*0} is the hadron energy in the fluid element rest frame, γ_s is strangeness suppression factor, quantum statistics is accounted for

$$\rho_i^{\text{eq}}(T, \mu_i) = \int_0^\infty d^3 \vec{p}^* f_i^{\text{eq}}(p^{*0}; T(x^*), \mu(x^*)_i) = 4\pi \int_0^\infty dp^* p^{*2} f_i^{\text{eq}}(p^{*0}; T, \mu_i)$$

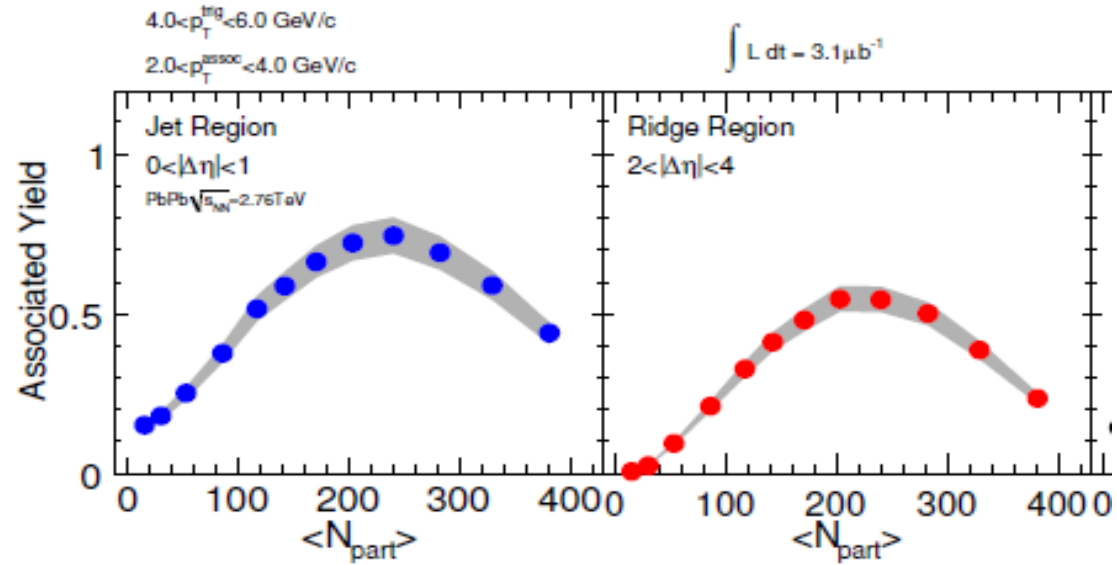
The mean multiplicity N_i of a hadron species i :

$$N_i = \rho_i(T, \mu_i) V_{\text{eff}} \quad P(N_i) = \exp(-\bar{N}_i) \frac{(\bar{N}_i)^{N_i}}{N_i!}$$

HYDJET++

data comparison, Integrated yield

CMS data, PAS HIN 11-006



Integrated associated yields in the near-side jet and ridge regions around, minus constant background (ZYAM method).

